

Research article

Open Access

## **Ab initio modeling of small proteins by iterative TASSER simulations**

Sitao Wu<sup>1</sup>, Jeffrey Skolnick<sup>2</sup> and Yang Zhang\*<sup>1</sup>

Address: <sup>1</sup>Center for Bioinformatics and Department of Molecular Bioscience, University of Kansas, 2030 Becker Dr, Lawrence, KS 66047, USA and <sup>2</sup>Center for the Study of Systems Biology, School of Biology, Georgia Institute of Technology, 250 14th Street NW, Atlanta, GA 30318, USA

Email: Sitao Wu - [stwu@ku.edu](mailto:stwu@ku.edu); Jeffrey Skolnick - [skolnick@gatech.edu](mailto:skolnick@gatech.edu); Yang Zhang\* - [yzhang@ku.edu](mailto:yzhang@ku.edu)

\* Corresponding author

Published: 8 May 2007

Received: 9 December 2006

*BMC Biology* 2007, **5**:17 doi:10.1186/1741-7007-5-17

Accepted: 8 May 2007

This article is available from: <http://www.biomedcentral.com/1741-7007/5/17>

© 2007 Wu et al; licensee BioMed Central Ltd.

This is an Open Access article distributed under the terms of the Creative Commons Attribution License (<http://creativecommons.org/licenses/by/2.0>), which permits unrestricted use, distribution, and reproduction in any medium, provided the original work is properly cited.

### **Abstract**

**Background:** Predicting 3-dimensional protein structures from amino-acid sequences is an important unsolved problem in computational structural biology. The problem becomes relatively easier if close homologous proteins have been solved, as high-resolution models can be built by aligning target sequences to the solved homologous structures. However, for sequences without similar folds in the Protein Data Bank (PDB) library, the models have to be predicted from scratch. Progress in the *ab initio* structure modeling is slow. The aim of this study was to extend the TASSER (threading/assembly/refinement) method for the *ab initio* modeling and examine systemically its ability to fold small single-domain proteins.

**Results:** We developed I-TASSER by iteratively implementing the TASSER method, which is used in the folding test of three benchmarks of small proteins. First, data on 16 small proteins (< 90 residues) were used to generate I-TASSER models, which had an average C<sub>α</sub>-root mean square deviation (RMSD) of 3.8Å, with 6 of them having a C<sub>α</sub>-RMSD < 2.5Å. The overall result was comparable with the all-atomic ROSETTA simulation, but the central processing unit (CPU) time by I-TASSER was much shorter (150 CPU days vs. 5 CPU hours). Second, data on 20 small proteins (< 120 residues) were used. I-TASSER folded four of them with a C<sub>α</sub>-RMSD < 2.5Å. The average C<sub>α</sub>-RMSD of the I-TASSER models was 3.9Å, whereas it was 5.9Å using TOUCHSTONE-II software. Finally, 20 non-homologous small proteins (< 120 residues) were taken from the PDB library. An average C<sub>α</sub>-RMSD of 3.9Å was obtained for the third benchmark, with seven cases having a C<sub>α</sub>-RMSD < 2.5Å.

**Conclusion:** Our simulation results show that I-TASSER can consistently predict the correct folds and sometimes high-resolution models for small single-domain proteins. Compared with other *ab initio* modeling methods such as ROSETTA and TOUCHSTONE II, the average performance of I-TASSER is either much better or is similar within a lower computational time. These data, together with the significant performance of automated I-TASSER server (the Zhang-Server) in the 'free modeling' section of the recent Critical Assessment of Structure Prediction (CASP)7 experiment, demonstrate new progresses in automated *ab initio* model generation. The I-TASSER server is freely available for academic users <http://zhang.bioinformatics.ku.edu/I-TASSER>.

## Background

Prediction of protein structure from amino-acid sequences has been one of the most challenging problems in computational structural biology for many years [1,2]. Historically, protein structure prediction was classified into three categories: (i) comparative modeling [3,4], (ii) threading [5-9], and (iii) *ab initio* folding [10-15]. The first two approaches build protein models by aligning query sequences onto solved template structures. When close templates are identified, high-resolution models could be built by the template-based methods. If templates are absent from the Protein Data Bank (PDB) library, the models need to be built from scratch, i.e. *ab initio* folding. This is the most difficult category of protein-structure prediction [16,17].

With increasing protein sizes, the conformational phase space of sampling also sharply increases, which makes the *ab initio* modeling of larger proteins extremely difficult [18]. Current *ab initio* predictions are mainly focused on small proteins. Several successful examples have been reported in literature. For example, based on an *ab initio* approach designed to globally optimize their potential energy function, Liwo et al were able to build models of  $C_\alpha$  root mean square deviation (RMSD) to native < 6Å for protein fragments of up to 61 residues [10]. Using the ROSETTA program [11], Simon et al reported 73 successful structure predictions out of 172 target proteins with lengths of < 150 residues, with  $C_\alpha$ -RMSD < 7Å in the top five models [19]. Using TOUCHSTONE-II software, Zhang et al reported 83 foldable cases from 125 target proteins (up to 174 residues) with  $C_\alpha$ -RMSD < 6.5Å in the top five models [12]. Recently, Bradley et al demonstrated an exciting achievement by building several high-resolution models for proteins of < 90 residues [13]. By combining low-resolution and high-resolution sampling, the authors used the all-atomic ROSETTA to predict high-resolution models with  $C_\alpha$ -RMSD < 1.5Å for 5 of 16 small proteins. The average  $C_\alpha$ -RMSD for all the 16 proteins was 3.8Å in the best of the top five clusters. The CPU time cost, however, is expensive and ~150 CPU days are required for the all-atom sampling of each target.

In this work, we aimed to investigate the possibility of generating high-resolution models of small proteins in an automated and fast simulation. We developed a new method, I-TASSER, which implements TASSER [18,20] in an iterative mode and also exploits new force-field optimization and fragment identification. We tested the I-TASSER method on three independent benchmark sets. The result shows that I-TASSER has a comparable overall performance with the all-atomic ROSETTA but with far lower CPU cost. It also demonstrates that I-TASSER clearly outperforms the TOUCHSTONE-II method.

## Results and discussion

We tested the folding performance of I-TASSER on small proteins. To avoid contamination with homologous proteins, any template with > 20% sequence identity to the target sequence was removed from our template library. Moreover, if a template could be detected by the Position Specific Iterative (PSI)-BLAST program with an E-value < 0.05, it would also be excluded. We note that the homology exclusion cutoff used here is more stringent than that used by Bradley et al [13], who only excluded templates with a PSI-BLAST E-value < 0.05 but without sequence identity cutoff, and that used by Zhang et al [12], who only excluded the templates with sequence identity > 30% but without PSI-BLAST checking. In the sense that all homologous templates had been completely excluded, we termed the corresponding simulations "*ab initio*" modeling, following the notation by others [10,12,13,21].

For the evaluation of the predicted models, we used both the RMSD and TM-score [22]. Although RMSD can give an explicit concept of modeling errors, in some cases, a local error (e.g., tail misorientation) can cause a large RMSD value even though the global topology is correct. TM-score is defined as [22].

$$\text{TM-score} = \frac{1}{N} \sum_{i=1}^{N_{ali}} \frac{1}{1 + (d_i/d_0)^2}, \quad (1)$$

where  $N$  is the number of residues of the query sequence and  $N_{ali}$  is the number of aligned residues in a threading alignment. For a full-length model,  $N$  and  $N_{ali}$  are identical.  $d_i$  is the distance of the  $i$ th  $C_\alpha$  pair between model and native after superposition, and  $d_0 = 1.24\sqrt[3]{N-15} - 1.8$ . As TM-score weights small distances stronger than larger distances, it is more sensitive to global topology than is RMSD. According to Zhang and Skolnick [22], TM-score = 1 indicates two identical structures and TM-score < 0.17 indicates random structure pairs. A TM-score of > 0.5 means two structures with the same folding.

### Benchmark I: 16 proteins from the data of Bradley et al

Table 1 shows the modeling result of I-TASSER on 16 small proteins that were used by Bradley et al [13]. This benchmark set includes 3  $\alpha$  proteins, 2  $\beta$  proteins, and 11  $\alpha\beta$  proteins with pairwise sequence identity < 30%. If we define a high-resolution model as that with  $C_\alpha$ -RMSD to native  $\leq 1.5\text{\AA}$ , I-TASSER predicts high-resolution models for one target 'logwA' (see Figure 2A for the model superimposed on the native structure). For the best of the top five clusters, most of the targets (12/16) had a medium resolution, with a  $C_\alpha$ -RMSD of 1.5–5Å. For the remaining three targets, I-TASSER could not correctly fold the pro-

teins. One of them (1tif\_) has a long swinging tail at the C-terminal. For the other two (1dcjA\_ and 1o2fB\_), both having a topology of four parallel  $\beta$ -strands flanked by two  $\alpha$ -helices, the imperfection of the I-TASSER force field is obviously responsible for the failure because the energy of the native structures is higher than that of the largest clusters.

For the first predicted model of the highest cluster density, the overall average  $C_{\alpha}$ -RMSD for the 16 target proteins was 4.3Å with average TM-score of 0.59. If we consider the best model in the top five predictions, the average  $C_{\alpha}$ -RMSD to the native is 3.8Å and TM-score was 0.61. Figure 2(b,c) shows typical examples of both medium-resolution and low-resolution predicted models.

As a comparison, the table also lists the all-atomic ROSETTA predictions for the 16 proteins (columns 4–6). ROSETTA predicted more high-resolution models than I-TASSER does. ROSETTA had three models < 1.5Å in round 1, four models in round 2, and two models in the top five clusters. The difference in the number of high-resolution models may indicate the resolution limitation of the reduced potential used in I-TASSER modeling. However, ROSETTA had more low-resolution models than did I-TASSER. If we define low-resolution models as those with a  $C_{\alpha}$ -RMSD > 5Å, ROSETTA had seven low-resolution models in round 1, five low-resolution models in round 2, and four low-resolution models in the best of the top five clusters. I-TASSER had only three low-resolution models in the best of the top five clusters. The overall average  $C_{\alpha}$ -RMSD of the best of the top five I-TASSER models is 3.8Å, comparable with that of ROSETTA (round 1: 5.1Å;

round 2: 4.7Å; top five: 3.8Å). The statistical equivalency of these two methods was at the 5% significance level under the Wilcoxon rank sum test based on  $C_{\alpha}$ -RMSD. However, the CPU time cost by I-TASSER was much shorter (~5 CPU hours vs. 150 CPU days). The main reason for the CPU saving might be that I-TASSER operates under reduced modeling, whereas the ROSETTA modeling is at an atomic level. The simulations on multiple homologous sequences also increase the computing time for ROSETTA [13].

Figure 3A shows the plot of  $C_{\alpha}$ -RMSD to native of the best model in the top five clusters versus that of the best threading alignments over the same aligned regions (star symbols). Almost all the final models (except 1b72A) were much closer to native than the best threading alignments, as indicated by the reduction of RMSD values. Along the same aligned region, the average  $C_{\alpha}$ -RMSD for the models and the templates were 3.6Å and 5.7Å respectively. The significant improvement of I-TASSER models on the threading alignments were also found here (Figure 3B), where the average TM-score for the models and the template were 0.61 and 0.49 respectively. Again, most of final models had a higher TM-score than that of the best threading alignments (a list of the best templates with the highest TM-score for each target protein in this study is available online at <http://zhang.bioinformatics.ku.edu/I-TASSER/templates>).

#### Benchmark II: 20 proteins from Zhang et al

In this benchmark set, we took 20 proteins from the data of Zhang et al [12]: six  $\alpha$ -proteins, six  $\beta$ -proteins, and eight  $\alpha\beta$ -proteins, with sizes ranging from 47 to 118 residues.

**Table 1: Summary of I-TASSER modeling on benchmark I in comparison with atomic ROSETTA [13]**

Protein name	Length (residues)	Secondary structure	$C_{\alpha}$ -RMSD (Å) of ROSETTA models			$C_{\alpha}$ -RMSD (Å) (TM-score) of I-TASSER models	
			Round 1	Round 2	Best in top five clusters	First cluster	Best in top five clusters
1b72A	49	$\alpha$	0.8	1.1	1.0	3.3 (0.64)	3.1 (0.64)
1shfA	59	$\beta$	11.1	10.8	10.9	1.7 (0.75)	1.7 (0.75)
1tif_	59	$\alpha\beta$	5.3	4.1	3.8	7.0 (0.33)	7.0 (0.36)
2reb_2	60	$\alpha\beta$	1.2	2.1	1.3	5.6 (0.37)	4.7 (0.57)
1r69_	61	$\alpha$	2.1	1.2	1.7	1.9 (0.75)	1.9 (0.75)
1csp_	67	$\beta$	5.1	4.7	5.1	2.1 (0.76)	2.1 (0.76)
1di2A_	69	$\alpha\beta$	2.6	2.6	1.9	2.3 (0.78)	2.3 (0.78)
1n0uA4	69	$\alpha\beta$	9.9	10.2	2.7	4.4 (0.48)	4.4 (0.48)
1mla_2	70	$\alpha\beta$	8.4	8.7	7.2	2.8 (0.66)	2.7 (0.66)
1af7_	72	$\alpha$	10.1	10.4	1.7	4.2 (0.49)	4.2 (0.49)
1ogwA_	72	$\alpha\beta$	2.7	1.0	2.6	1.1 (0.88)	1.1 (0.88)
1dcjA_	73	$\alpha\beta$	3.2	2.5	2.0	10.5 (0.39)	10.0 (0.39)
1dtjA_	74	$\alpha\beta$	1.0	1.2	1.8	1.9 (0.80)	1.7 (0.82)
1o2fB_	77	$\alpha\beta$	10.1	N/A	10.3	7.1 (0.41)	5.2 (0.43)
1mkyA3	81	$\alpha\beta$	3.2	6.3	3.7	5.2 (0.40)	4.5 (0.50)
1tig_	88	$\alpha\beta$	4.1	3.5	2.4	7.7 (0.50)	4.4 (0.54)
Average	69		5.1	4.7	3.8	4.3 (0.59)	3.8 (0.61)

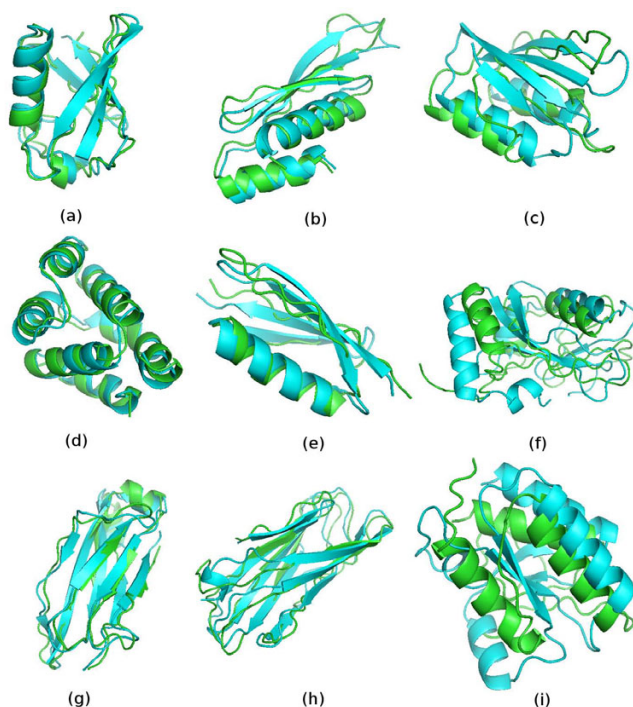


**Figure 2**  
**Examples of I-TASSER models from three independent benchmark sets.** The green color is for I-TASSER models and blue for the native structures. (A–C) are from benchmark I (Bradley et al [13]); (D–F) are from benchmark II (Zhang et al [12]); and (G–I) are from benchmark III, selected directly from the PDB library. Column 1 contains the high-resolution models with a  $C_{\alpha}$ -RMSD  $\leq 1.5\text{\AA}$ ; column 2 contains the medium-resolution models with a  $C_{\alpha}$ -RMSD of  $1.5\text{--}5\text{\AA}$ ; column 3 contains the low-resolution models with a  $C_{\alpha}$ -RMSD  $> 5\text{\AA}$ . The  $C_{\alpha}$ -RMSD value for the examples are: **(A)** logwA\_ (1.1 $\text{\AA}$ ), **(B)** ldi2A\_ (2.3 $\text{\AA}$ ), **(C)** ldcjA\_ (10.0 $\text{\AA}$ ), **(D)** lcy5A (1.5 $\text{\AA}$ ), **(E)** lpgx (3.1 $\text{\AA}$ ), **(F)** lgnuA (8.2 $\text{\AA}$ ), **(G)** lcqkA (1.5 $\text{\AA}$ ), **(H)** lgyvA (3.3 $\text{\AA}$ ), **(I)** lno5A (10.5 $\text{\AA}$ ). The pictures were generated using PyMOL software [45].

These 20 proteins were selected so that they and the proteins used in benchmark I had pairwise sequence identity of  $< 30\%$ .

As shown in Table 2, in this benchmark set, most of the targets had medium resolution, with  $C_{\alpha}$ -RMSD to native of  $1.5\text{--}5\text{\AA}$  by I-TASSER. More specifically, for the best of the top five clusters, 14 targets had medium resolution, 5 targets had low resolution, and 1 target (lcy5A) had high resolution. Typical examples from the three categories are shown in Figure 2(D–F). The comparisons of the final models with the initial threading alignments are shown in

Figure 3 (A,B; circles). Again, the global topology of the final models was significantly closer to the native structure than were the threading alignments. The average  $C_{\alpha}$ -RMSD and TM-score of the initial threading alignments were 6.1 $\text{\AA}$  and 0.53 respectively, but after I-TASSER simulations, they improved to 3.4 $\text{\AA}$  and 0.65.

Compared with the TOUCHSTONE-II modeling [12], I-TASSER predicted better models in 17 cases, with lower  $C_{\alpha}$ -RMSD in the best of the top 5 clusters. Only in three cases did I-TASSER models have slightly higher  $C_{\alpha}$ -RMSD, i.e. 1bq9A (5.0 $\text{\AA}$  vs. 4.8 $\text{\AA}$ ), 256bA (3.4 $\text{\AA}$  vs. 3.2 $\text{\AA}$ ), and 2pcy\_ (4.6 $\text{\AA}$  vs. 4.3 $\text{\AA}$ ). The overall average  $C_{\alpha}$ -RMSD results for the TOUCHSTONE-II and I-TASSER models were 5.9 $\text{\AA}$  and 3.9 $\text{\AA}$  respectively. Statistically, the result of I-TASSER was better than that of TOUCHSTONE-II at the 1% significance level using the Wilcoxon rank sum test.

The algorithm of TOUCHSTONE-II was previously developed in our group, and searches for protein conformations on a cubic lattice system. Each residue in TOUCHSTONE-II is represented by its  $C_{\alpha}$ ,  $C_{\beta}$ , and the side-chain center of mass (the CABS model [12]). The force field consists of a variety of knowledge-based statistical potentials from PDB and the side-chain contact restraints predicted by PROSPECTOR\_3 [9]. In TASSER [20], we assemble the protein models directly using the continuous fragments from the PROSPECTOR\_3 alignment, in which the conformations are searched in an "on-and-off" lattice system, i.e. the threading-aligned regions are modeled off-lattice and the unaligned loop regions on-lattice. Each residue is represented by the  $C_{\alpha}$  and the side-chain center of mass (the CAS model [20]). The force field was developed from TOUCHSTONE-II, with new potentials including the sequence-specified pair-wise potential [23],  $C_{\alpha}$  distance correlations from sequence-specific fragments [20], and the more accurate secondary structure-specified hydrogen bonding [24]. The force field of I-TASSER is mainly developed from that of TOUCHSTONE-II and TASSER. The new components in I-TASSER include: (i) the new neural network hydrophobic potential as described in equation 3 in the Methods section and the decoy-based reparameterization of all weight-factors based on target categories; (ii) the development of the new PPA threading program, which provides different assembly fragments and restraints; and (iii) the two-step iterative refinement simulations. For conformational sampling, the introduction of the on-and-off lattice fragment assembly simulation in TASSER and I-TASSER is the key factor to speed up the search of important phase spaces because the usage of rigid-body fragments dramatically reduces the entropy of the searched space. The modeling improvement data shown in Table 3 demonstrates the progress of I-TASSER in both potentials and sampling since TOUCHSTONE-II [12].

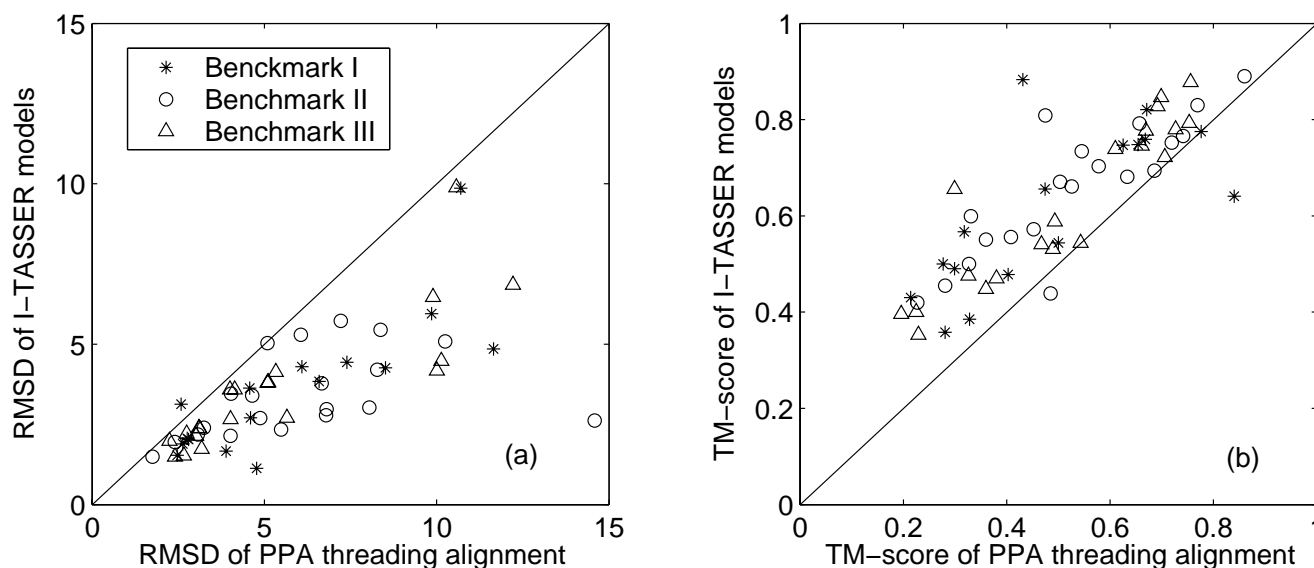


**Figure 3**  
**Comparison of I-TASSER models with the PPA threading alignment results. (A)**  $C_{\alpha}$ -RMSD to native of the I-TASSER models versus  $C_{\alpha}$ -RMSD to native of the best threading alignment over the same aligned regions. **(B)** TM-score of the I-TASSER models versus TM-score of the best threading alignments.

#### **Benchmark III: 20 non-homologous small proteins selected from the PDB**

For the testing of the generality of I-TASSER folding on small proteins, we constructed the third benchmark proteins directly from the PDB library. As listed in Table 3, this set includes seven  $\alpha$ -proteins, six  $\beta$ -proteins, and seven  $\alpha\beta$ -proteins, with lengths ranging from 56 to 118 residues. To avoid the redundancy of the benchmarks, the proteins were selected so that this set and the previously used 36 target proteins had sequence identity between all the pairs of < 30%. The proteins were randomly taken from PDB, but the targets with unusual topology (such as coiled-coil or a structure with a long tail) were excluded.

The average  $C_{\alpha}$ -RMSD of the best in top five models by I-TASSER was 3.9Å (4.8Å for rank 1 models), which was similar to that of benchmarks I and II. Again, there was one model (1cqkA) with a high-resolution prediction, as presented in Figure 2g. There were 14 medium-resolution predictions and 5 low-resolution ones. The typical examples from these two categories are shown in Figure 2(H and I). The global topology of the final models was also markedly closer to the native structure than the threading alignments, as shown in Figure 3 (triangle symbols). Overall, the model quality and the  $C_{\alpha}$ -RMSD distribution in this independent set was comparable with the benchmark sets taken from Bradley et al [13] and Zhang et al [12], which demonstrates the robustness and stability of the I-TASSER modeling on *ab initio* small-protein folding. The I-TASSER method was also tested in recent blind

CASP7 experiments [25], where the overall TM-score of the I-TASSER models was significantly better than that of all other automated methods (>5% higher than the second-best CASP7 server).

#### **Conclusion**

In summary, we have developed a new approach to protein structure modeling by iteratively implementing the TASSER method. Meanwhile, we have introduced a new profile-profile alignment approach for the I-TASSER fragment collection, and a new neural network-trained hydrophobic potential, which has been implemented in a reduced Monte Carlo simulation for the first time.

The benchmark proteins were taken from three independent sources, in which any solved structure that had a sequence identity of > 20% to the targets and could be detected by PSI-BLAST with an E-value of < 0.05 was removed from the template library.

The I-TASSER folding showed comparable overall results with the all-atomic ROSETTA simulation, especially in the medium-resolution region. It is noteworthy that, even with reduced modeling, the current I-TASSER has the capacity to generate high-resolution models, although the frequency of high-resolution cases was lower than that of the all-atomic ROSETTA. Further development of the atomic potential for the I-TASSER might be helpful in increasing the modeling accuracy in the high-resolution region, but it would certainly increase the CPU cost of I-

**Table 2: Summary of I-TASSER modeling on benchmark II in comparison with TOUCHSTONE-II [12]**

Protein name	Length (residues)	Secondary structure	$C_{\alpha}$ -RMSD (Å) of TOUCHSTONE-II models		$C_{\alpha}$ -RMSD (Å) (TM-score) of I-TASSER models	
			Best in top five clusters	First cluster	Best in top five clusters	First cluster
lgpt_	47	$\alpha\beta$	4.0	5.2 (0.54)	3.8 (0.56)	4.0 (0.57)
ltfi_	47	$\beta$	6.2	4.6 (0.56)	4.0 (0.57)	4.0 (0.57)
lbq9A	53	$\beta$	4.8	7.3 (0.41)	5.0 (0.46)	5.0 (0.46)
lpgx_	59	$\alpha\beta$	6.0	3.1 (0.55)	3.1 (0.55)	3.1 (0.55)
lah9_	63	$\beta$	5.1	4.3 (0.56)	2.8 (0.67)	2.8 (0.67)
laoy_	65	$\alpha$	4.7	4.5 (0.70)	2.7 (0.70)	2.7 (0.70)
lsro_	71	$\beta$	4.3	3.4 (0.66)	3.0 (0.68)	3.0 (0.68)
lkjs_	74	$\alpha$	8.2	8.5 (0.38)	5.7 (0.50)	5.7 (0.50)
lvcc_	76	$\alpha\beta$	7.3	5.7 (0.44)	5.7 (0.44)	5.7 (0.44)
lnpsA	88	$\alpha\beta$	3.4	2.1 (0.79)	2.1 (0.79)	2.1 (0.79)
lhbka	89	$\alpha$	8.5	3.5 (0.69)	3.5 (0.69)	3.5 (0.69)
lcy5A	92	$\alpha$	1.8	1.5 (0.89)	1.5 (0.89)	1.5 (0.89)
lbn8_	99	$\alpha\beta$	9.0	6.3 (0.42)	6.3 (0.42)	6.3 (0.42)
2pcy_	99	$\beta$	4.3	4.6 (0.66)	4.6 (0.66)	4.6 (0.66)
256bA	106	$\alpha$	3.2	3.4 (0.77)	3.4 (0.77)	3.4 (0.77)
lcewl	108	$\alpha\beta$	6.3	3.6 (0.73)	3.6 (0.73)	3.6 (0.73)
lthx_	108	$\alpha\beta$	2.3	2.1 (0.83)	2.1 (0.83)	2.1 (0.83)
lsfp_	111	$\beta$	6.0	5.1 (0.75)	5.1 (0.75)	5.1 (0.75)
lgnuA	117	$\alpha\beta$	9.3	8.2 (0.58)	6.5 (0.60)	6.5 (0.60)
2a0b_	118	$\alpha$	12.8	2.5 (0.81)	2.5 (0.81)	2.5 (0.81)
Average	85		5.9	4.5 (0.64)	3.9 (0.65)	3.9 (0.65)

TASSER. Currently, the average CPU time for small proteins is about 5 CPU hours for I-TASSER, whereas the CPU cost for the atomic ROSETTA modeling is 150 CPU days per target.

The I-TASSER modeling results obviously outperform those generated by TOUCHSTONE-II [12], with the average  $C_{\alpha}$ -RMSD reducing from 5.9Å to 3.9Å for the same protein set. As the sequence identity cutoff used here was more stringent than that used by TOUCHSTONE-II, the improvement demonstrates the progress of I-TASSER in both force field and conformational sampling.

Although the benchmark proteins were taken from different sources, the overall performance of I-TASSER was very similar. For the first predicted models, the average  $C_{\alpha}$ -RMSD ranged from 4.3Å to 4.8Å and the average TM-score ranged from 0.59 to 0.64 for the three benchmarks. For the best models in the top five predictions, the average  $C_{\alpha}$ -RMSD ranged from 3.8Å to 3.9Å and the average TM-score ranged from 0.61 to 0.65. This modeling stability, along with the consistent results from I-TASSER server in the "free modeling" section of the recent CASP7 experiment, demonstrates the robustness of I-TASSER method in predicting correct folds for small proteins. Meanwhile, the capacity of generating medium-resolution to high-resolution models using reduced modeling represents new progress in the field of *ab initio* modeling.

## Methods

The I-TASSER method is an extension of the previous TASSER (threading/assembly/refinement) method [18,20]. The overall procedure is described in Figure 1. This method has also been used in the automated server section, named 'Zhang-Server', in the recent CASP7 experiment.

### PPA threading

The query sequence is first threaded through the PDB library [26] to identify appropriate local fragments, which will be adopted for further structural reassembly. The threading method used in I-TASSER is a simple profile-profile alignment (PPA) approach. The alignment score between the  $i$ th residue of the query sequence and the  $j$ th residue of the template structure is defined as

$$Score(i, j) = \sum_{k=1}^{20} P_{query}(i, k) L_{template}(j, k) + c_1 \delta(s_{query}(i), s_{template}(j)) + c_2 \quad (2)$$

where  $P_{query}(i, k)$  is the frequency of the  $k$ th amino acid at the  $i$ th position of the query sequence when a PSI-BLAST [27] search of the query sequence runs against a non-redundant sequence database <ftp://ftp.ncbi.nih.gov/blast/db/nr.00.tar.gz> and <ftp://ftp.ncbi.nih.gov/blast/db/nr.01.tar.gz> with an E-value cutoff of 0.001;  $L_{template}(j, k)$  is the log-odds profile of template sequence in the PSI-BLAST search;  $S_{query}(i)$  is the secondary structure prediction from PSIPRED [28] for the  $i$ th residue of the query

**Table 3: Summary of I-TASSER modeling on the Benchmark III**

Protein name	Length (residues)	Secondary structure	$C_{\alpha}$ -RMSD (Å) (TM-score) of I-TASSER models	
			First cluster	Best in top five clusters
I ne3A	56	$\beta$	4.6 (0.45)	4.6 (0.48)
2cr7A	60	$\alpha$	4.5 (0.48)	2.6 (0.66)
2f3nA	65	$\alpha$	1.8 (0.74)	1.8 (0.74)
l itpA	68	$\alpha\beta$	10.9 (0.33)	4.5 (0.40)
l kviA	68	$\alpha\beta$	2.0 (0.72)	2.0 (0.72)
l b4bA	71	$\alpha\beta$	6.4 (0.48)	5.6 (0.54)
l gjxA	77	$\beta$	6.9 (0.44)	5.6 (0.47)
l of9A	77	$\alpha$	3.6 (0.53)	3.6 (0.53)
l mn8A	84	$\alpha$	7.0 (0.35)	7.0 (0.35)
l fo5A	85	$\alpha\beta$	3.8 (0.54)	3.8 (0.54)
l ten_	87	$\beta$	1.6 (0.85)	1.6 (0.85)
l fadA	92	$\alpha$	3.6 (0.59)	3.6 (0.59)
l no5A	93	$\alpha\beta$	10.6 (0.43)	10.5 (0.45)
l g l cA	98	$\beta$	2.5 (0.79)	2.5 (0.79)
l cqkA	101	$\beta$	1.5 (0.88)	1.5 (0.88)
l abv_	103	$\alpha$	13.0 (0.28)	6.8 (0.40)
l jnuA	104	$\alpha\beta$	2.7 (0.75)	2.7 (0.75)
l egxA	115	$\alpha\beta$	2.3 (0.80)	2.3 (0.83)
l gyvA	117	$\beta$	3.3 (0.78)	3.3 (0.78)
l orgA	118	$\alpha$	2.4(0.78)	2.4(0.78)
Average	87		4.8 (0.60)	3.9 (0.63)

sequence and  $S_{template}(j)$  the secondary structure assignment by DSSP [29] for the  $j$ th residue of the template. The weight factor  $c_1$  is an adjustable parameter for balancing the profile term and the secondary structure matches; the shift constant  $c_2$  is introduced to avoid the alignment of unrelated regions in the local alignment [8]. The Needleman-Wunsch dynamic programming algorithm [30] is used to find the best match between query and template sequences. A position-dependent gap penalty is used: no gap is allowed inside the secondary structure regions; gap opening ( $c_3$ ) and gap extension ( $c_4$ ) penalties apply to other regions; and the ending gap penalty is ignored. The best tuning parameters, based on our trial and error on the ProSup benchmark [31], are:  $c_1 = 0.6$ ,  $c_2 = 1.0$ ,  $c_3 = 7.0$ ,  $c_4 = 0.5$ .

### Structure assembly

A protein chain in the I-TASSER modeling is divided into aligned and unaligned regions based on the PPA alignment, where the aligned regions are modeled off-lattice for maximum accuracy of the secondary structure blocks and the unaligned regions are simulated on a cubic lattice system for computational efficiency [20].

For a given alignment, an initial full-length model is built up by connecting the continuous secondary structure fragments ( $\geq 5$  residues) through a random walk of  $C_{\alpha}$ - $C_{\alpha}$  bond vectors of variable lengths from 3.26 to 4.35Å. Only excluded volume and geometric constraints of virtual  $C_{\alpha}$ - $C_{\alpha}$  bond angles (65–165°) are considered during the ini-

tial model-building procedure. The side-chain center of mass is determined by a two-rotamer approximation that depends on whether the local backbone configuration is extended or compact. To guarantee that the last step of this random walk can quickly arrive at the first  $C_{\alpha}$  of the next template fragment, the distance  $l$  between the current  $C_{\alpha}$  and the first  $C_{\alpha}$  of the next template fragment is checked at each step of the random walk, and only walks with  $l < 3.54n$  are allowed, where  $n$  is the number of remaining  $C_{\alpha}$ - $C_{\alpha}$  bonds in the walk. If a template gap is too big to span by a specified number of unaligned residues, a big  $C_{\alpha}$ - $C_{\alpha}$  bond will remain at the end of the random walk and a spring-like force that acts to draw sequential fragments close will be applied in subsequent Monte Carlo simulations until a physically reasonable bond length is achieved.

The initial full-length models are submitted to parallel-exchange Monte Carlo sampling [32] for assembly/refinement. Two kinds of conformational updates (off-lattice and on-lattice) are implemented. (i) Off-lattice movements of the aligned regions involve rigid fragment translations and rotations that are controlled by the three Euler angles. The fragment length normalizes the movement amplitude so that the acceptance rate is approximately constant for fragments with different sizes. (ii) The lattice-confined residues are subjected to 2–6 bond movements and multi-bond sequence shifts [12]. Overall, the tertiary topology varies by the rearrangement of the continuously aligned substructures, where the local conformation of



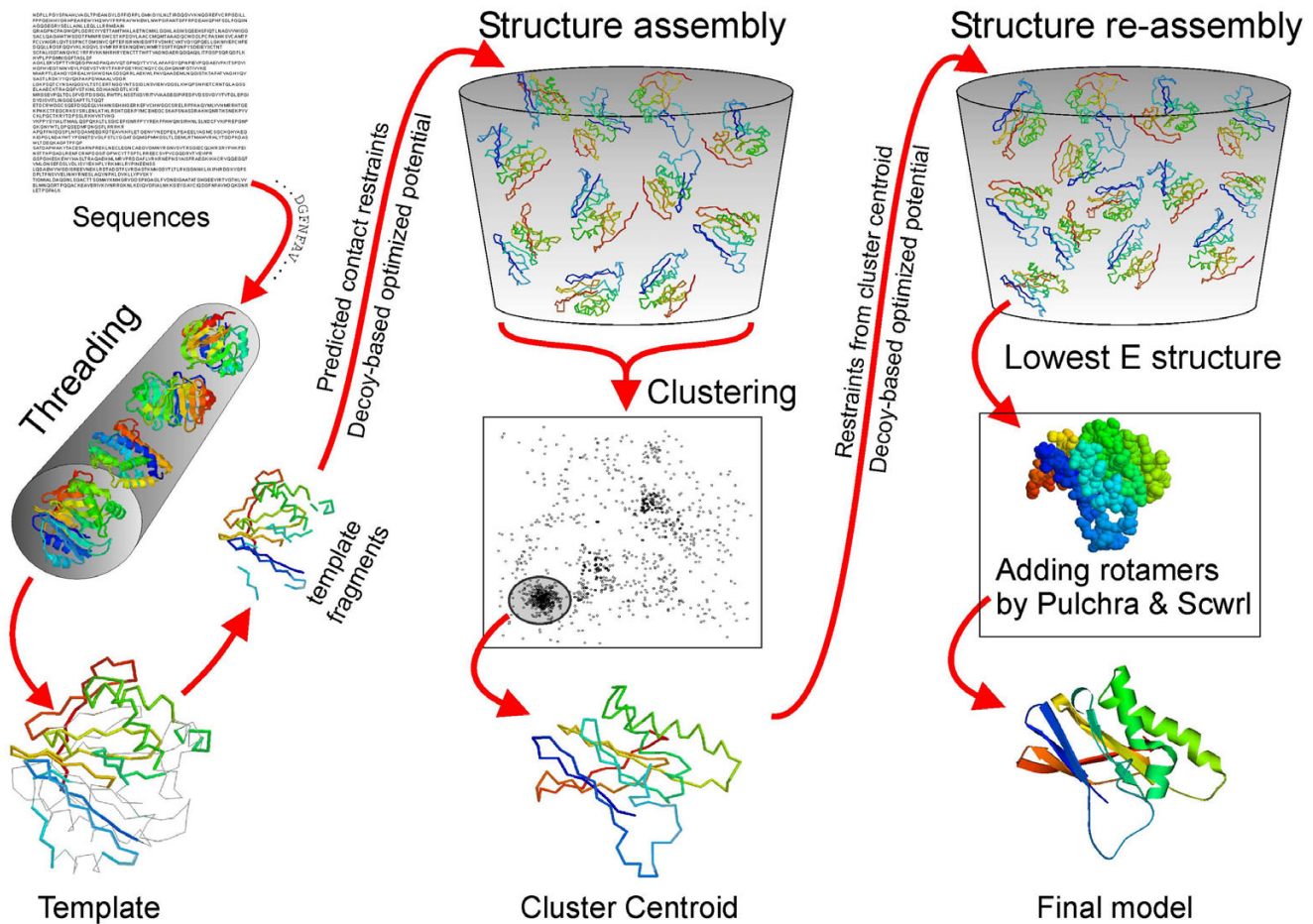


**Figure 1**  
Flowchart of I-TASSER method for protein structure prediction.

the off-lattice substructures remains unchanged during assembly.

**Force field**

The inherent I-TASSER assembly force field is similar to TASSER, which includes predicted secondary structure propensities from PSIPRED [28], backbone hydrogen bonds [24], and a variety of statistical short-range and long-range correlations [12,18,20]. The major new potential in I-TASSER is the incorporation of the predicted accessible surface area (ASA) through the neural network (NN) [33].

For the purpose of fast calculations of the ASA effect, the hydrophobic energy in I-TASSER is defined by

$$E_{ASA} = -\sum_i \left( \frac{x_i^2}{x_0^2} + \frac{y_i^2}{y_0^2} + \frac{z_i^2}{z_0^2} - 2.5 \right) * P(i), \quad (3)$$

where  $(x_i, y_i, z_i)$  is the coordinate of  $i$ th residue at the ellipsoid Cartesian system of the given protein conformation and  $(x_0, y_0, z_0)$  is the principle axes length. Thus, 2.5 is a suitable parameter to tune the average depth of the exposed residues. The two-state (expose/bury) neural network was trained on 3365 non-redundant high-resolution protein structures on the basis of their sequence profile from PSI-BLAST [27]. The maximum ASA value in an extended tripeptide (Ala-X-Ala) is taken from Ahmad et al [34]. Twelve different ASA fraction cutoffs (0.05, 0.1, ... 0.6) are used to define the residue expose status in the NN



training. The residue expose index is  $P(i) = \sum_{j=1}^{12} a_j$ , where  $a_j$  is the two-state neural network prediction of exposure ( $a_j = 1$ ) or burial ( $a_j = -1$ ) with the  $j$ th ASA fraction cutoff, which has a strong correlation with the real value of ASA. For an independent set of 2234 non-homologous proteins used by Zhang and Skolnick [18,20], the overall correlation coefficient between the predicted  $P(i)$  and the real exposed area assigned by STRIDE [35] is 0.71, whereas the same correlation for the widely-used Hopp-Woods [36] and Kyte-Doolittle [37] hydrophobicity indices are 0.42 and 0.39 respectively. One of the reasons for the higher correlation is that NN prediction explores the sequence-profile information, whereas the Hopp-Woods and Kyte-Doolittle parameters are sequence-independent.

### Second-round TASSER simulation

The structure trajectories of the first-round TASSER simulations are clustered by SPICKER [38]. The cluster centroids are obtained by averaging all the clustered structures after superposition, which generally have substantial steric clashes and can be over-compressed [39]. Following the clustering, the TASSER Monte Carlo simulation is implemented again, and this starts from the cluster centroid conformations (see Figure 1). The distance and contact restraints in the second-round TASSER are taken from the combination of the centroid structures and the PDB structures searched by the structure alignment program TM-align [40] based on the cluster centroids. The conformation with the lowest energy in the second round is selected. Finally, Pulchra [41] is used to add backbone atoms (N, C, O) and Scwrl\_3.0 [42] is used to build side-chain rotamers. The sidechain-building procedure by Pulchra and Scwrl does not modify the  $C_\alpha$  coordinates.

At this point, one of the main purposes of the second-round TASSER is to remove the steric clashes of the cluster centroids. Based on a benchmark test of 200 proteins < 300 residues in size (unpublished data), after the second round of TASSER, the average number of steric clashes for the first cluster reduces from 79 to 0.8. Here, a clash is defined as a pair of residues with  $C_\alpha$  distance < 3.6Å [43]. For the PDB experimental structures, the average number of steric clashes for the 200 proteins is 0.46, which is close to that of the second-round TASSER models. However, as strong distance and contact restraints have been implemented in the second-round simulation, the topology improvement of the models is modest. For the 200 test proteins, the average TM-score [22] increases from 0.5734 to 0.5801 (1.2%) and  $C_\alpha$ -RMSD to native decreases from 6.67Å to 6.52Å compared with the cluster centroid of the first round. Another option of removing the steric clashes is simply to use a TASSER decoy closest to the cluster cen-

teroid, but in that case, the average TM-score decreases to 0.5583 (by 2.7%) and  $C_\alpha$ -RMSD to native increases to 7.15Å.

We also tried MODELLER [3] and NEST [44] softwares to refine the centroid models. In both cases, the average  $C_\alpha$ -RMSD was increased in comparison with the cluster centroids. In particular, these tools cannot entirely remove the steric clashes. For the 200 test cases, the average numbers of remaining steric clashes of MODELLER and NEST models were 16.7 and 22.6 respectively.

### Authors' contributions

SW, JS, and YZ developed the I-TASSER method and drafted the paper. SW collected benchmark protein sets, carried out I-TASSER simulations, and performed data analysis. All authors read and approved the final manuscript.

### Acknowledgements

We thank Dr Huilin Chen for the discussion of the neural network training of the ASA prediction and help in using the neural network program. The work was finished on the KU ITTC computer cluster, and the assistance of Drs Victor Frost and Adam Hock are gratefully acknowledged. The project was partially supported by KU Start-up Fund 06194 and NFGRF 2302003.

### References

- Baker D, Sali A: **Protein structure prediction and structural genomics.** *Science* 2001, **294(5540)**:93-96.
- Skolnick J, Fetrow JS, Kolinski A: **Structural genomics and its importance for gene function analysis.** *Nat Biotechnol* 2000, **18(3)**:283-287.
- Sali A, Blundell TL: **Comparative protein modelling by satisfaction of spatial restraints.** *J Mol Biol* 1993, **234(3)**:779-815.
- Fiser A, Do RK, Sali A: **Modeling of loops in protein structures.** *Protein Sci* 2000, **9(9)**:1753-1773.
- Bowie JU, Luthy R, Eisenberg D: **A method to identify protein sequences that fold into a known three-dimensional structure.** *Science* 1991, **253**:164-170.
- Jones DT, Taylor WR, Thornton JM: **A new approach to protein fold recognition.** *Nature* 1992, **358(6381)**:86-89.
- Xu Y, Xu D: **Protein threading using PROSPECT: design and evaluation.** *Proteins* 2000, **40(3)**:343-354.
- Zhou H, Zhou Y: **Fold recognition by combining sequence profiles derived from evolution and from depth-dependent structural alignment of fragments.** *Proteins* 2005, **58(2)**:321-328.
- Skolnick J, Kihara D, Zhang Y: **Development and large scale benchmark testing of the PROSPECTOR 3.0 threading algorithm.** *Protein* 2004, **56**:502-518.
- Liwo A, Lee J, Ripoll DR, Pillardy J, Scheraga HA: **Protein structure prediction by global optimization of a potential energy function.** *Proceedings of the National Academy of Sciences of the United States of America* 1999, **96(10)**:5482-5485.
- Simons KT, Kooperberg C, Huang E, Baker D: **Assembly of protein tertiary structures from fragments with similar local sequences using simulated annealing and Bayesian scoring functions.** *J Mol Biol* 1997, **268(1)**:209-225.
- Zhang Y, Kolinski A, Skolnick J: **TOUCHSTONE II: A new approach to ab initio protein structure prediction.** *Biophysical journal* 2003, **85**:1145-1164.
- Bradley P, Misura KM, Baker D: **Toward high-resolution de novo structure prediction for small proteins.** *Science* 2005, **309(5742)**:1868-1871.
- Klepeis JL, Wei Y, Hecht MH, Floudas CA: **Ab initio prediction of the three-dimensional structure of a de novo designed protein: a double-blind case study.** *Proteins* 2005, **58(3)**:560-570.

15. Klepeis JL, Floudas CA: **ASTRO-FOLD: a combinatorial and global optimization framework for Ab initio prediction of three-dimensional structures of proteins from the amino acid sequence.** *Biophys J* 2003, **85(4)**:2119-2146.
16. Skolnick J, Kolinski A: **A unified approach to the prediction of protein structure and function.** *Adv Chem Phys* 2002, **120**:131-192.
17. Floudas CA, Fung HK, McAllister SR, Monnigmann M, Rajgaria R: **Advances in Protein Structure Prediction and De Novo Protein Design: A Review.** *Chemical Engineering Science* 2006, **61**:966-988.
18. Zhang Y, Skolnick J: **Tertiary structure predictions on a comprehensive benchmark of medium to large size proteins.** *Biophysical journal* 2004, **87**:2647-2655.
19. Simons KT, Strauss C, Baker D: **Prospects for ab initio protein structural genomics.** *J Mol Biol* 2001, **306**:1191-1199.
20. Zhang Y, Skolnick J: **Automated structure prediction of weakly homologous proteins on a genomic scale.** *Proceedings of the National Academy of Sciences of the United States of America* 2004, **101**:7594-7599.
21. Simons KT, Ruczinski I, Kooperberg C, Fox BA, Bystruff C, Baker D: **Improved recognition of native-like protein structures using a combination of sequence-dependent and sequence-independent features of proteins.** *Proteins* 1999, **34**:82-95.
22. Zhang Y, Skolnick J: **Scoring function for automated assessment of protein structure template quality.** *Proteins* 2004, **57**:702-710.
23. Zhang Y, Skolnick J: **The protein structure prediction problem could be solved using the current PDB library.** *Proceedings of the National Academy of Sciences of the United States of America* 2005, **102**:1029-1034.
24. Zhang Y, Hubner I, Arakaki A, Shakhnovich E, Skolnick J: **On the origin and completeness of highly likely single domain protein structures.** *Proceedings of the National Academy of Sciences of the United States of America* 2006, **103**:2605-2610.
25. Zhang Y: **Protein structure prediction by I-TASSER at CASP7.** *Invited talk given at CASP7 conference: 2006; Asilomar Conference Center, Pacific Grove, CA* 2006.
26. Berman HM, Westbrook J, Feng Z, Gilliland G, Bhat TN, Weissig H, Shindyalov IN, Bourne PE: **The Protein Data Bank.** *Nucleic acids research* 2000, **28**:235-242.
27. Altschul SF, Madden TL, Schaffer AA, Zhang J, Zhang Z, Miller W, Lipman DJ: **Gapped BLAST and PSI-BLAST: a new generation of protein database search programs.** *Nucleic acids research* 1997, **25**:3389-3402.
28. Jones DT: **Protein secondary structure prediction based on position-specific scoring matrices.** *J Mol Biol* 1999, **292**:195-202.
29. Kabsch W, Sander C: **Dictionary of protein secondary structure: pattern recognition of hydrogen-bonded and geometrical features.** *Biopolymers* 1983, **22**:2577-2637.
30. Needleman SB, Wunsch CD: **A general method applicable to the search for similarities in the amino acid sequence of two proteins.** *J Mol Biol* 1970, **48(3)**:443-453.
31. Domingues FS, Lackner P, Andreeva A, Sippl MJ: **Structure-based evaluation of sequence comparison and fold recognition alignment accuracy.** *J Mol Biol* 2000, **297(4)**:1003-1013.
32. Zhang Y, Kihara D, Skolnick J: **Local energy landscape flattening: Parallel hyperbolic Monte Carlo sampling of protein folding.** *Proteins* 2002, **48**:192-201.
33. Chen H, Zhou HX: **Prediction of solvent accessibility and sites of deleterious mutations from protein sequence.** *Nucleic acids research* 2005, **33(10)**:3193-3199.
34. Ahmad S, Gromiha MM, Sarai A: **Real value prediction of solvent accessibility from amino acid sequence.** *Proteins* 2003, **50(4)**:629-635.
35. Frishman D, Argos P: **Knowledge-based protein secondary structure assignment.** *Proteins* 1995, **23(4)**:566-579.
36. Hopp TP, Woods KR: **Prediction of protein antigenic determinants from amino acid sequences.** *Proc Natl Acad Sci USA* 1981, **78**:3824-3828.
37. Kyte J, Doolittle RF: **A simple method for displaying the hydropathic character of a protein.** *J Mol Biol* 1982, **157(105-132)**.
38. Zhang Y, Skolnick J: **SPICKER: A clustering approach to identify near-native protein folds.** *J Comput Chem* 2004, **25(6)**:865-871.
39. Zhang Y, Arakaki A, Skolnick J: **TASSER: An automated method for the prediction of protein tertiary structures in CASP6.** *Proteins* 2005, **61(Suppl 7)**:91-98.
40. Zhang Y, Skolnick J: **TM-align: a protein structure alignment algorithm based on the TM-score.** *Nucleic acids research* 2005, **33(7)**:2302-2309.
41. Feig M, Rotkiewicz P, Kolinski A, Skolnick J, Brooks CL 3rd: **Accurate reconstruction of all-atom protein representations from side-chain-based low-resolution models.** *Proteins* 2000, **41(1)**:86-97.
42. Canutescu AA, Shelenkov AA, Dunbrack RL Jr: **A graph-theory algorithm for rapid protein side-chain prediction.** *Protein Sci* 2003, **12(9)**:2001-2014.
43. Tress M, Ezkurdia I, Grana O, Lopez G, Valencia A: **Assessment of predictions submitted for the CASP6 comparative modeling category.** *Proteins* 2005, **61(Suppl 7)**:27-45.
44. Petrey D, Xiang Z, Tang CL, Xie L, Gimpelev M, Mitros T, Soto CS, Goldsmith-Fischman S, Kernysky A, Schlessinger A, et al.: **Using multiple structure alignments, fast model building, and energetic analysis in fold recognition and homology modeling.** *Proteins* 2003, **53(Suppl 6)**:430-435.
45. Delano WL: **(Delano Scientific, San Carlos, CA, USA, 2002).**

Publish with **BioMed Central** and every scientist can read your work free of charge

"BioMed Central will be the most significant development for disseminating the results of biomedical research in our lifetime."

Sir Paul Nurse, Cancer Research UK

Your research papers will be:

- available free of charge to the entire biomedical community
- peer reviewed and published immediately upon acceptance
- cited in PubMed and archived on PubMed Central
- yours — you keep the copyright

Submit your manuscript here:  
[http://www.biomedcentral.com/info/publishing\\_adv.asp](http://www.biomedcentral.com/info/publishing_adv.asp)

